Chapter 22
A Review of Magnetic Phenomena in Probe-Brane Holographic Matter

Oren Bergman, Johanna Erdmenger, and Gilad Lifschytz

22.1 Introduction

The behavior of strongly interacting matter subject to background magnetic fields is an interesting and physically relevant problem in many different scenarios, ranging from the effective 2d electron gas in graphene, to magnetars, which are neutron stars with a strong magnetic field. Magnetic fields give rise to a rich array of phenomena. Some examples in QCD are the magnetic catalysis of chiral symmetry breaking [1–3], anomaly-driven phases of baryonic matter [4], and the chiral magnetic effect [5]. It has also been suggested that magnetic fields induce ρ-meson condensation and superconductivity in the QCD vacuum [6, 7]. There are also many interesting examples in condensed matter physics, most notably the fractional quantum Hall effect [8, 9].

Gauge/gravity duality, also known as holographic duality, has emerged in recent years as a particularly useful approach to strong-coupling dynamics. Although it does not seem to be directly applicable to physical systems, this approach can be used to study theoretical systems that exhibit the same type of phenomena, and that capture some of the relevant physics. The techniques of holographic duality are especially efficient in addressing questions associated with finite temperature and density, background fields and transport properties, that are difficult to study

O. Bergman (✉)
Technion, Israel Institute of Technology, Haifa 32000, Israel
e-mail: bergman@physics.technion.ac.il

J. Erdmenger
Max Planck Institute for Physics, 80805 Munich, Germany
e-mail: jke@mppmu.mpg.de

G. Lifschytz
Department of Mathematics and Physics, University of Haifa at Oranim, Tivon 36006, Israel
e-mail: giladl@research.haifa.ac.il

D. Kharzeev et al. (eds.), *Strongly Interacting Matter in Magnetic Fields*,
Lecture Notes in Physics 871, DOI 10.1007/978-3-642-37305-3_22,

using other non-perturbative methods. This approach can also lead to new ideas for constructing effective theories of the physical phenomena one is interested in.

Holographic models are divided into two main types, commonly referred to as top-down models and bottom-up models. In top-down models the bulk gravitational description of the system corresponds to a consistent solution of a well-defined quantum gravity theory, either in the context of the full string theory or in terms of the low-energy effective supergravity theory. This then defines some particular strong-coupling boundary dynamics. In bottom-up models, on the other hand, one builds into the description what one needs in order to produce the desired boundary dynamics. Each approach has advantages and disadvantages. Top-down models are more firmly grounded than bottom-up models, however they are more restrictive in terms of the variety and scope of phenomena they can exhibit.

Probe-brane models are a class of top-down holographic models, in which matter fields transforming in the fundamental representation of a gauge group are incorporated by embedding "flavor" D-branes in the gravitational background dual to the gauge theory [10]. These branes are treated as probes, in the sense that we neglect their backreaction on the background. (This corresponds to the 'quenched' approximation in the dual gauge theory, where matter loops are neglected in computing gluon amplitudes.) The matter fields are manifest in this construction: they correspond to the open strings between the flavor branes and the "color" branes that make up the background. In particular, one can easily design probe brane models in which the light matter degrees of freedom are purely fermionic, which is obviously a desirable feature for many physical systems, including QCD and condensed matter electron systems.

The matter dynamics is determined by the properties of the probe brane embedding. In particular, the fluctuations of the probe brane worldvolume fields correspond to gauge-invariant composite operators that describe the mesonic states of the matter system. There are generically two types of embeddings at finite temperature: "BH embeddings", in which the brane extends to the horizon of the background, and "MN embeddings", in which the brane terminates outside the horizon. The two embedding types describe different phases of the matter in the dual gauge theory. For example, in the MN phase the mesons are stable since they are associated with real eigenfrequencies of the probe brane fluctuations. In the BH phase, on the other hand, some of the energy of the fluctuations is dissipated into the black hole, leading to complex eigenfrequencies and damping. In this case the mesons have a finite lifetime. MN embeddings are favored at low temperature, and as the temperature is increased one generically observes a first order phase transition to a BH embedding.

The most extensively studied probe-brane models are the D3–D7 model [10], in which D7-branes are added to the D3-brane background, and the D4–D8 (or Sakai-Sugimoto) model [11], in which D8-branes and anti-D8-branes are added to the background of D4-branes compactified on a circle. Both models describe a strongly-coupled gauge theory in four dimensions with fundamental matter degrees of freedom, and both exhibit a number of phenomena similar to QCD. More recently, a different D3–D7 system, more closely related to the D4–D8 system, has been used as a model of strongly-interacting fermionic matter in three spacetime di-

mensions [12–15]. We will refer to this as the D3–D7' model. This model exhibits several interesting phenomena that are familiar in planar condensed matter systems.

Probe-brane models are especially well-designed to study the properties of the dual matter systems at non-zero density and in background electromagnetic fields. Both are implemented by turning on specific components of the probe-brane world-volume gauge field, and solving the resulting coupled differential equations for the embedding and the gauge fields. Here one observes another basic difference between the two types of embeddings in terms of their response to a background electric field. MN embeddings correspond to electrical insulators with a mass-gap to charged excitations, and BH embeddings describe gapless conductors.

Probe-brane models also exhibit a number of interesting phenomena in a background magnetic field, which are qualitatively similar to the phenomena listed in the beginning. In this paper we will review how each of the three models mentioned above respond at non-zero density to a background magnetic field in various situations. In particular, we will encounter the magnetic catalysis effect in both the D3–D7 and D4–D8 models. In the D3–D7 model we will also demonstrate the formation of a superfluid state. In the D4–D8 model we will describe anomaly-generated currents and baryonic states, as well as a metamagnetic-like transition. In the D3–D7' model we will see both quantum and anomalous Hall effects, as well as how the magnetic field influences the instability to the formation of stripes, and the zero-sound mode.

This paper is divided into three main sections, reviewing each of the probe-brane models in turn. For completeness let us mention that magnetic fields also play an important role in the related D3–D5 system, where the probe D5-brane corresponds to additional $(2+1)$-dimensional degrees of freedom in the dual gauge theory. In this model, the magnetic field leads to a phase transition of Berezinskii-Kosterlitz-Thouless (BKT) type [16, 17]. For brevity we do not discuss this model in this review.

22.2 The D3–D7 Model

22.2.1 Brane Construction

The starting point for this model is the usual configuration of the AdS/CFT correspondence [18] which involves a stack of N D3 branes. This has an open string interpretation in which the low-energy degrees of freedom are described by $U(N)$ $\mathcal{N}=4$ super-Yang-Mills theory. On the other hand, in the closed string interpretation of N D3 branes, the low-energy *near-horizon* limit gives rise to the space $AdS_5 \times S^5$. Identifying the two pictures leads to the AdS/CFT correspondence.

Let us now add N_f probe D7-branes to this configuration, as first done in [10] and reviewed in detail in [19]. Within $(9+1)$-dimensional flat space, the D3-branes are extended along the 0123 directions, whereas the D7-branes are extended along the 01234567 directions. This configuration preserves $1/4$ of the total amount of

supersymmetry in type IIB string theory (corresponding to 8 real supercharges) and has an $SO(4) \times SO(2)$ isometry in the directions transverse to the D3-branes. The $SO(4)$ rotates x^4, x^5, x^6, x^7, while the $SO(2)$ group acts on x^8, x^9. Separating the D3-branes from the D7-branes in the $(8, 9)$ directions by a distance l explicitly breaks the $SO(2)$ group. These geometrical symmetries are also present in the dual field theory: The dual field theory is an $\mathcal{N} = 2$ supersymmetric $(3+1)$-dimensional theory in which the degrees of freedom of $\mathcal{N} = 4$ super-Yang-Mills theory are coupled to N_f hypermultiplets of flavor fields with fermions and scalars (ψ_i, q^n), $i = 1, 2$, $n = 1, 2$, which transform in the fundamental representation of the gauge group. Separating the D7-branes from the D3-branes corresponds to giving a mass to the hypermultiplets.

For massless flavor fields, the Lagrangian is classically invariant under conformal transformations $SO(4, 2)$.[1] Moreover, the theory is invariant under the R-symmetries $SU(2)_R$ and $U(1)_R$ as well as under the global $SU(2)_\Phi$, which rotates the scalars in the adjoint hypermultiplet. Note that the mass term in the Lagrangian breaks the $U(1)_R$ symmetry explicitly. If all N_f flavor fields have the same mass m, the field theory is invariant under a global $U(N_f)$ flavor group. The baryonic $U(1)_B$ symmetry is a subgroup of the $U(N_f)$ flavor group. These symmetries of the field theory side may be identified with symmetries of the D3–D7 brane intersection and hence also with the dual gravity description.

For this field theory, gauge invariant composite operators may now be constructed which transform in suitable representations of the $SU(2) \times SU(2) \times U(1)$ symmetry group isomorphic to the geometrical $SO(4) \times SO(2)$. These operators are expected to be dual to the fluctuations of the D7-brane which transform in the same representation, as worked out in detail in [20]. An example of a meson operator is given by

$$\mathcal{M}^A = \bar{\psi}_i \sigma^A{}_{ij} \psi_j + \bar{q}^m X^A q^m, \quad (i, m = 1, 2), \tag{22.1}$$

with X^A the vector (X^8, X^9) of adjoint scalars associated with the $(8, 9)$ directions, and $\sigma^A \equiv (\sigma^1, \sigma^2)$ a doublet of Pauli matrices. Thus (22.1) has charge $+2$ under $U(1)_R$. It is a singlet under both $SU(2)_\Phi$ and $SU(2)_R$. The conformal dimension is $\Delta = 3$. This operator may be viewed as a supersymmetric generalization of a mesonic operator in QCD, with the index A labeling two scalar mesons.

The standard AdS/CFT duality relates the $\mathcal{N} = 4$ super-Yang-Mills degrees of freedom to supergravity on $AdS_5 \times S^5$. In addition, there are new degrees of freedom associated to the D7-brane worldvolume fields originating from the open strings on the D7-brane. The additional duality maps these to the mesonic operators in the field theory. This is an open-open string duality, as opposed to the standard AdS/CFT correspondence, which is an open-closed string duality. The dynamics of the D7-brane is described by the Dirac-Born-Infeld (DBI) action

[1] However note that the scale-invariance is broken at the quantum level since the beta function is proportional to N_f/N_c and therefore non-vanishing. In the limit $N_c \to \infty$ with N_f being fixed, the beta function is approximately zero, i.e. we may treat the theory as being scale invariant also at the quantum level.

$$S_{D7} = -\frac{\mu_7}{g_s}\int d^8\xi\,\sqrt{-\det\bigl(G_{ab}+B^{(2)}_{ab}+2\pi\alpha' F_{ab}\bigr)}, \tag{22.2}$$

where $\mu_7 = [(2\pi)^7\alpha'^4]^{-1}$. G and $B^{(2)}$ are the induced metric and two-form field on the probe brane worldvolume, and F_{ab} is the worldvolume field strength. The D7-brane action also contains a fermionic term S^f_{D7}. In addition there may also be contributions of Wess-Zumino form. An example for this will be discussed below.

Let us write the $AdS_5 \times S^5$ metric in the form

$$ds^2 = \frac{r^2}{R^2}\eta_{ij}\,dx^i\,dx^j + \frac{R^2}{r^2}\bigl(d\rho^2 + \rho^2\,d\Omega_3^2 + dx_8^2 + dx_9^2\bigr), \tag{22.3}$$

with $i, j = 0, 1, 2, 3$, $\rho^2 = x_4^2 + \cdots + x_7^2$, $r^2 = \rho^2 + x_8^2 + x_9^2$ and R the AdS radius. Since the D7-brane is transverse to x_8, x_9 in flat space, we see that it extends along AdS_5 and wraps an S^3 inside S^5 in the near-horizon background. The action for a static D7-brane embedding, for which F_{ab} may be consistently set to zero on its world-volume, is given from (22.2) up to angular factors by

$$S_{D7} = -\frac{\mu_7}{g_s}\int d^8\xi\,\rho^3\sqrt{1+\dot{x}_8^2+\dot{x}_9^2}, \tag{22.4}$$

where a dot indicates a ρ derivative (*e.g.* $\dot{x}_8 \equiv \partial_\rho x_8$). The ground state configuration of the D7-brane then corresponds to the solution of the equation of motion

$$\frac{d}{d\rho}\left[\frac{\rho^3}{\sqrt{1+\dot{x}_8^2+\dot{x}_9^2}}\frac{dx}{d\rho}\right] = 0, \tag{22.5}$$

where x denotes either x_8 or x_9. Clearly the action is minimized by x_8, x_9 being any arbitrary constant. Therefore the embedded D7-brane is flat. According to string theory, the choice of the position in the x_8, x_9 plane corresponds to choosing the quark mass in the gauge theory action. The fact that x_8, x_9 are constant at all values of the radial coordinate ρ, which corresponds to the holographic renormalization scale, may be interpreted as non-renormalization of the mass in the dual field theory.

In general, the equations of motion have asymptotic ($\rho \to \infty$) solutions of the form

$$x = l + \frac{c}{\rho^2} + \cdots, \tag{22.6}$$

where l is related to the quark mass m by

$$m = \frac{l}{2\pi\alpha'}. \tag{22.7}$$

In agreement with the standard AdS/CFT result about the asymptotic behavior of supergravity fields near the boundary, the parameter c must correspond to the vev of an operator with the same symmetries as the mass and of dimension three, since ρ carries energy dimension. c is therefore a measure of the quark condensate $\bar{\psi}\psi$.

c is obtained from $\partial\mathscr{L}/\partial m$ which in addition to the fermion bilinear also includes scalar squark terms. We may consistently assume that the squarks have zero vev. Moreover, supersymmetry requires that a vev for c must be absent since c is an F-term of a chiral superfield: $\tilde{\psi}\psi$ is the F-term of $\tilde{Q}Q$. Supersymmetry is broken if $c = \langle\tilde{\psi}\psi\rangle \neq 0$. This is reflected also in the supergravity solution: The solutions to the supergravity equations of motion with c non-zero are not regular in AdS space and are therefore excluded.

We therefore consider the regular supersymmetric embeddings of the D7-brane for which the quark mass m may be non-zero, but the condensate c vanishes. For massive embeddings, the D7-brane is separated from the stack of D3-branes in either the x_8 or x_9 directions, where the indices refer to the coordinates given in (22.3). In this case the radius of the S^3 becomes a function of the radial coordinate r in AdS_5. At a radial distance from the deep interior of the AdS space given by the hypermultiplet mass, the radius of the S^3 shrinks to zero. From a five-dimensional AdS point of view, this gives a minimal value for the radial coordinate r beyond which the D7-brane cannot extend further. This is in agreement with the induced metric on the D7-brane world-volume, which is given by

$$ds^2 = \frac{\rho^2 + l^2}{R^2}\eta_{ij}\,dx^i\,dx^j + \frac{R^2}{\rho^2 + l^2}\,d\rho^2 + \frac{R^2\rho^2}{\rho^2 + l^2}\,d\Omega_3{}^2, \tag{22.8}$$

$$d\Omega_3{}^2 = d\psi^2 + \cos^2\psi\,d\beta^2 + \sin^2\psi\,d\gamma^2, \tag{22.9}$$

where $\rho^2 = r^2 - l^2$ and Ω_3 are spherical coordinates in the 4567-space. For $\rho \to \infty$, this is the metric of $AdS_5 \times S^3$. When $\rho = 0$ (*i.e.* $r^2 = l^2$), the radius of the S^3 shrinks to zero.

22.2.2 Finite Temperature

The finite temperature system is realized holographically by placing the D7-brane in an AdS-Schwarzschild black hole background with metric given by

$$ds^2 = \frac{r^2}{2R^2}\left(\frac{d\mathbf{x}^2({r_h}^4 + r^4)}{r^4} - \frac{dt^2(r^4 - {r_h}^4)^2}{r^4({r_h}^4 + r^4)}\right) + \frac{R^2}{r^2}\left(dL^2 + d\rho^2 + L^2\,d\phi^2 + \rho^2\,d\Omega_3^2\right), \tag{22.10}$$

where $r^2 = \rho^2 + L^2$. The temperature is given by $T = r_h/(\pi R^2)$.

In this metric we have introduced polar coordinates (L, ϕ) in the (x_8, x_9) plane and consider solutions for D7-brane embeddings with $L = L(\rho)$, $\phi = \text{const}$. The asymptotic near-boundary behavior of these brane embeddings is given by

$$L(\rho) = l + \frac{c}{\rho^2} + \cdots, \tag{22.11}$$

where $m = l/(2\pi\alpha')$ is the bare quark mass and c is proportional to the condensate $\langle\bar{\psi}\psi\rangle$. At finite temperature, supersymmetry is broken and brane embeddings with c non-zero are possible, in contrast to the supersymmetric case discussed above.

Depending on the quark mass, there are two different types of embeddings: Those which reach the black hole, and those which do not since the S^3 they wrap shrinks to zero outside the black hole horizon. The first type of branes is referred to as 'black hole' (BH) embeddings, while the second type is referred to as 'Minkowski' (MN) embeddings. In the BH case, fluctuations of the probe brane have complex eigenfrequencies or quasi-normal modes, which means that the mesons associated with these fluctuations decay. In the MN phase, the mesons are stable. The phase transition between the two types of embeddings is first order.

At finite temperature, the solution with $m = 0$ also has $c = 0$. However, in gravity backgrounds corresponding to confining field theories, brane embeddings with $m = 0$, $c \neq 0$ are possible. These realize spontaneous chiral symmetry breaking [21].

22.2.3 Magnetic Catalysis

Let us now consider, as was first done in [22], a magnetic field induced by a pure gauge B-field in the worldvolume direction of the D3-branes,

$$B^{(2)} = B\, dx^2 \wedge dx^3, \tag{22.12}$$

which satisfies $dB^{(2)} = 0$. This contributes to the DBI action (22.2). Since $B^{(2)}$ and $2\pi\alpha' F$ enter (22.2) in the same way, we may trade $B^{(2)}$ for a gauge field on the probe brane via $F = -B^{(2)}/2\pi\alpha'$, which justifies interpreting B of (22.12) as a magnetic field.

In addition, there is a non-trivial Wess-Zumino contribution to the action, which at first order in α' is of the form

$$S_{\rm WZ} = 2\pi\alpha'\mu_7 \int F \wedge C^{(6)}. \tag{22.13}$$

In the presence of the B-field, this leads to an additional non-trivial contribution to the action, as explained in detail in [22]. This gives rise to a non-trivial $C^{(6)}$ which breaks supersymmetry on the worldvolume of the D7-brane.

Since supersymmetry is broken, the D7-brane now has a profile which depends on ρ as in (22.11), even at zero temperature. The Lagrangian corresponding to (22.2) takes the form

$$\mathscr{L} = -\frac{\mu_7}{g_s}\rho^3 \sin\psi\cos\psi\sqrt{1+L'^2}\sqrt{1+\frac{R^4B^2}{(\rho^2+L^2)^2}}. \tag{22.14}$$

For $m = 0$, the brane embedding solution obtained from this Lagrangian has non-zero $c \propto \langle\bar{\psi}\psi\rangle$ in (22.11). The magnetic field therefore induces spontaneous chiral

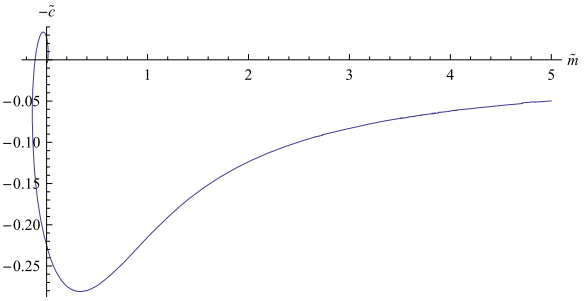

Fig. 22.1 $-\tilde{c}(\tilde{m})$ at vanishing temperature, with $-\tilde{c} = \langle\bar{\psi}\psi\rangle(2\pi\alpha')^3/(R^3B^{3/2})$, $\tilde{m} = m(2\pi\alpha')/(R\sqrt{B})$. Reproduced from [23]

symmetry breaking, a phenomenon known as *magnetic catalysis* [1–3]. For large m, the condensate may be calculated analytically [22] and is found to be

$$\langle\bar{\psi}\psi\rangle \propto -c = -\frac{R^4}{4l}B^2. \tag{22.15}$$

For small m, c has to be evaluated numerically. The result is shown in Fig. 22.1. By evaluating the free energy, it has been shown that when there is more than one solution, the one with the larger condensate is preferred.

At small values of the magnetic field, it is possible to analytically evaluate the shift of the meson masses due to its presence. For fluctuations of the embedding scalar in particular, a Zeeman splitting is observed [22]. While in the absence of a magnetic field, in the supersymmetric case described here, the scalar meson mass obtained from the fluctuations is $M_0(n) = 2m/\sqrt{\lambda}\cdot\sqrt{(n+1)(n+2)}$ [20], for non-zero magnetic field there is a mass splitting

$$M_\pm = M_0 \pm \frac{1}{\sqrt{\lambda}}\frac{B}{m}. \tag{22.16}$$

A review of magnetic catalysis in probe D7-brane systems is given in [24]. Magnetic catalysis is also found in systems involving N_f D7 branes where the back-reaction of the metric on the background geometry is taken into account [25–27]. Out-of-equilibrium dynamics associated with the phase transition induced by magnetic catalysis has been investigated in [28].

In the finite temperature case, there is a competition between two mechanisms: The black hole attracts the D7-brane, while it is repelled at small radii by the magnetic field. This implies a phase transition between a phase where the D7-brane reaches the black hole and one where it does not. This is shown in Fig. 22.2 for different values of the magnetic field, where the dimensionless ratio B/T^2 is used. A detailed discussion of the normalization is found in [23].

There is a critical value for B/T^2 above which the probe brane is repelled from the black hole for all values of the bare quark mass: In this case, chiral symmetry is spontaneously broken and the mesons are stable. The phase diagram is shown in Fig. 22.3.

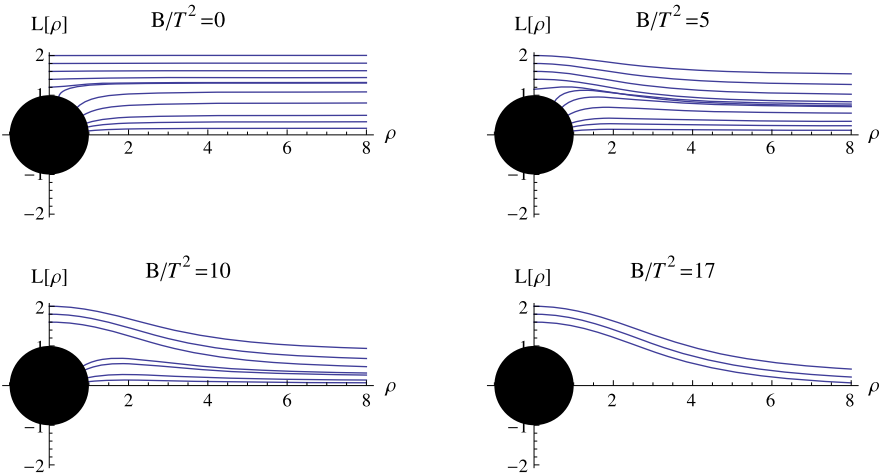

Fig. 22.2 Increasing values of B/T^2 for fixed T show the repulsive nature of the magnetic field. We see that for large enough B/T^2, the melted phase is never reached, and the chiral symmetry is spontaneously broken. Figure reproduced from [23]

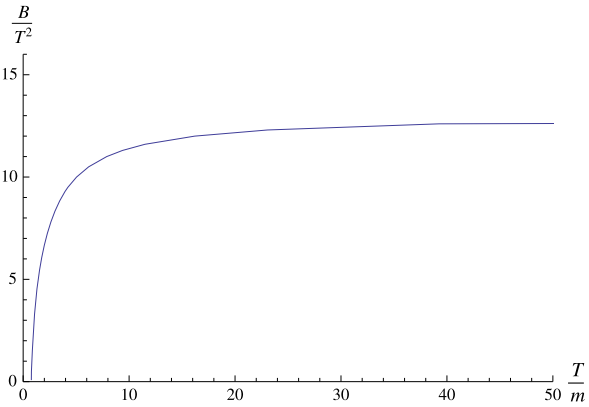

Fig. 22.3 Phase diagram for the D3/D7 system in the $(B/T^2, T/m)$ plane. Figure from [23]

More involved phase diagrams are obtained if a $U(1)$ chemical potential and density are turned on in addition to the magnetic field by considering a non-trivial profile for the $U(1)$ gauge field on the D7-brane [29–31]. An example of a phase diagram is shown in Fig. 22.4.

22.2.4 Superfluid

At finite isospin density, the D3–D7 model realizes a holographic superfluid [32, 33]. Finite isospin density is obtained by considering two coincident D7-branes, and using an ansatz for solving the equations of motion, which involves a non-trivial

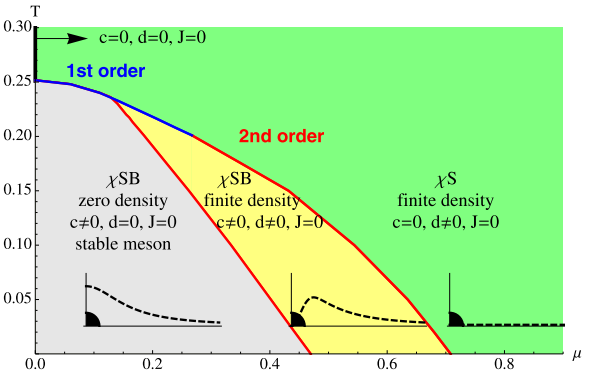

Fig. 22.4 Phase transitions at constant B field in the (T, μ) plane for the D3/D7 model. Figure reproduced from [31] by kind permission of the authors. c, d, J refer to the condensate, density and electric current, respectively

profile for the temporal component of the $SU(2)$ worldvolume gauge field, with asymptotic behavior

$$A^3{}_t(\rho) \propto \mu^3 + \frac{d^3}{\rho^2}. \tag{22.17}$$

μ^3 breaks the $SU(2)$ symmetry explicitly to a residual $U(1)_3$. In the presence of this background, the energetically favored solution also involves a non-trivial spatial component of the worldvolume gauge field,

$$A^1{}_x(\rho) \propto \frac{d^1{}_x}{\rho^2}. \tag{22.18}$$

Here the leading contribution is absent in the asymptotic behavior, so the $U(1)_3$ symmetry is spontaneously broken. $A^1{}_x$ is dual to a condensate of the form

$$d^1{}_x \propto \left\langle \bar{\psi}\sigma^1\gamma_x\psi + \bar{\phi}\sigma^i\partial_x\phi \right\rangle, \tag{22.19}$$

which is the supersymmetric equivalent of the ρ meson. The calculation of the frequency-dependent conductivity $\sigma(\omega)$ for this solution shows that it describes a superfluid: $\sigma(\omega)$ displays a gap. For the Sakai-Sugimoto model discussed below, a similar condensation mechanism has been found in [34] and superfluidity has been discussed in [35].

As discussed in [36, 37], a similar condensation process also happens when the profile (22.17) for the *temporal* component of the $SU(2)$ gauge field is replaced by a non-trivial profile for a *spatial* component of the form

$$A^3{}_x = By, \tag{22.20}$$

which corresponds to a background magnetic field. In this case a similar condensation as above takes place. This has been demonstrated by analyzing the fluctuations about the magnetic field background [37]: The quasi-normal modes of particular fluctuations cross into the upper half of the complex frequency plane above a critical value of the magnetic field, indicating an instability. This is shown in Fig. 22.5.

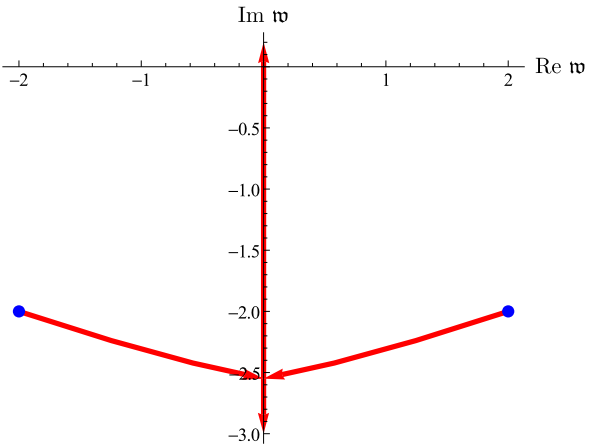

Fig. 22.5 Quasi-normal modes cross into the upper half plane above a critical magnetic field, signaling an instability. Figure reproduced from [37]

Finally let us note that the Hall conductivity has been calculated for the D3/D7 model in [38]. Unlike the isospin case, the ground state involving the ρ condensate is spatially modulated for the magnetic field background, leading to an Abrikosov lattice [39]. A similar ρ meson condensation mechanism in a background magnetic field has been found in the context of field theory in [6, 7, 40], based on similar earlier results in electroweak theory [41]. For the Sakai-Sugimoto model which we discuss below, a similar mechanism has been discussed in [42, 43].

22.3 The D4–D8 (Sakai-Sugimoto) Model

22.3.1 Basics

N_c D4-branes on $\mathbb{R}^{1,3} \times S^1$ with anti-periodic boundary conditions for fermions provide a holographic model for the low energy behavior of 4d $SU(N_c)$ Yang-Mills theory with $g_{YM}^2 = 4\pi g_s \sqrt{\alpha'}/R_4$ [44]. The near-horizon background at zero temperature is given by (we work with dimensionless coordinates rescaled by R)

$$\begin{aligned} ds^2_{con} &= u^{\frac{3}{2}}\left(-dx_0^2 + d\mathbf{x}^2 + f(u)\,dx_4^2\right) + u^{-\frac{3}{2}}\left(\frac{du^2}{f(u)} + u^2\,d\Omega_4^2\right), \\ e^{\Phi} &= g_s u^{3/4}, \qquad F_4 = 3\pi\left(\alpha'\right)^{3/2} N_c\; d\Omega_4, \end{aligned} \tag{22.21}$$

where $f(u) = 1 - (u_{KK}^3/u^3)$, $u_{KK} = 4R^2/(9R_4^2)$ and $R = (\pi g_s N_c)^{1/3}\sqrt{\alpha'}$. The IR "wall" at $u = u_{KK}$ implies that the dual gauge theory is confining. At nonzero temperature there is another possible background with a metric

$$ds^2_{dec} = u^{\frac{3}{2}}\left(-f(u)\,dx_0^2 + d\mathbf{x}^2 + dx_4^2\right) + u^{-\frac{3}{2}}\left(\frac{du^2}{f(u)} + u^2\,d\Omega_4^2\right), \tag{22.22}$$

where $f(u) = 1 - (u_T^3/u^3)$ and $u_T = (4\pi/3)^2 R^2 T^2$. This background becomes the dominant one when $T > 1/(2\pi R_4)$. The presence of a horizon at $u = u_T$ in this background indicates that the gauge theory undergoes a (first order) deconfinement transition at this temperature.

Quarks are added to the model by including D8-branes and anti-D8-branes that are localized on the circle [11]. With N_f D8-branes at one point and N_f anti-D8-branes at another point, the model has N_f flavors of massless right-handed and left-handed fermions, and a $U(N_f)_R \times U(N_f)_L$ chiral symmetry. The 8-branes are treated as probes in the near horizon background of the D4-branes. The flavor dynamics is thus encoded in the 5d effective worldvolume theory of the D8-branes, which includes a DBI term and a CS term (in Lorentzian signature)[2]

$$S_{DBI} = -\mathcal{N} \int d^4x\, du\, u^{1/4} \sqrt{-\det(g_{MN} + f_{MN})}, \tag{22.23}$$

$$S_{CS} = -\frac{\mathcal{N}}{8} \int d^4x\, du\, \varepsilon^{MNPQR} a_M f_{NP} f_{QR}. \tag{22.24}$$

The dimensionless worldvolume gauge field a_M and field strength f_{MN} are defined as $a_M = (2\pi\alpha'/R)A_M$ and $f_{MN} = 2\pi\alpha' F_{MN}$, and the overall normalization is given by $\mathcal{N} = \mu_8 \Omega_4 R^9/g_s = (1/3)N_c\, R^6 (2\pi)^{-5} (\alpha')^{-3}$. The anti-D8-brane has a similar action in terms of its worldvolume gauge field $\bar{a}_M$. The DBI term is identical to that of the D8-brane, and the CS term has the opposite sign. We define the vector combination as $a_M^V = \frac{1}{2}(a_M + \bar{a}_M)$, and the axial combination as $a_M^A = \frac{1}{2}(\bar{a}_M - a_M)$.

In the low-temperature confining background (22.21) the D8-brane and anti-D8-brane connect at $u = u_0 \geq u_{KK}$ into a smooth U-shaped configuration (Fig. 22.6a), reflecting the spontaneous breaking of the $U(1)_R \times U(1)_L$ chiral symmetry to the diagonal $U(1)_V$. The embedding is determined by the DBI action (setting $f_{MN} = 0$)

$$S_{DBI}^{con} = -\mathcal{N} \int d^4x\, du\, u^4 \left[f(u) \big(x_4'(u)\big)^2 + \frac{1}{u^3 f(u)} \right]^{\frac{1}{2}}, \tag{22.25}$$

which implies an asymptotic behavior

$$x_4(u) \approx \frac{L}{2} - \frac{2}{9} \frac{u_0^4 \sqrt{f(u_0)}}{u^{9/2}}, \tag{22.26}$$

where L is the asymptotic brane-antibrane separation.

The normalizable fluctuations of the D8-brane worldvolume fields in this embedding correspond to the (low spin) mesons of the model. Their mass scale is set by u_0, which we can think of as the mass of a "constituent quark" described by an open string from u_0 to u_{KK}. There is one massless pseudoscalar field φ, precisely as one

[2] For simplicity, we will consider the single flavor case with one D8-brane and one anti-D8-brane. This does not affect any of the results qualitatively.

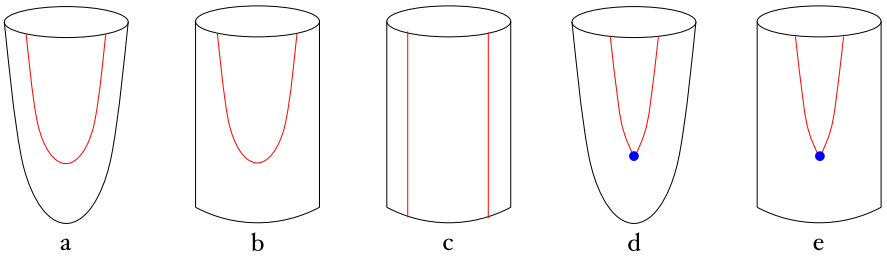

Fig. 22.6 D8-brane embeddings in the Sakai-Sugimoto model: **(a)** confined vacuum, **(b)** deconfined vacuum, **(c)** deconfined plasma, **(d)** confined nuclear matter, **(e)** deconfined nuclear matter

expects from the broken chiral symmetry. This is related to the η' meson in QCD. It appears (in a gauge with $a_u = 0$) as the zero mode a_μ^A:[3]

$$a_\mu^A\big(x^\mu, u\big) = -\partial_\mu \varphi\big(x^\mu\big)\psi_0(u) + \text{higher modes}, \tag{22.27}$$

where

$$\psi_0(u) = \frac{2}{\pi}\arctan\sqrt{\frac{u^3}{u_{KK}^3} - 1}. \tag{22.28}$$

Baryons are described by D4-branes wrapped on S^4 inside the D8-brane. Their charge comes from the N_c strings which must be attached to the wrapped D4-brane to cancel a tadpole due to the background RR field. These strings end on the D8-brane, giving N_c units of charge.[4]

In the high-temperature deconfining background (22.22) the D8-branes and anti-D8-branes can be either connected (Fig. 22.6b) or disconnected, with $x_4(u) = L/2$ (Fig. 22.6c), the latter corresponding to the restoration of the chiral symmetry [46]. The DBI action in the high-temperature deconfining background is very similar:

$$S_{DBI}^{dec} = -\mathcal{N}\int d^4x\, du\, u^4\left[f(u)\big(x_4'(u)\big)^2 + \frac{1}{u^3}\right]^{\frac{1}{2}}. \tag{22.29}$$

Consequently the properties of the U embedding in this background are qualitatively similar to those of the embedding in the confining background, for example in terms of the spectrum of mesons. In the disconnected embedding there are no normaliz-

[3]Note that, although the boundary value is non-zero, this is a normalizable mode since the field strength is normalizable. Ordinarily, boundary values of bulk fields correspond to parameters in the boundary theory. But in this case there is a possible ambiguity, since the boundary value of a_μ^A can also describe a non-trivial gradient of the pseudoscalar field.

[4]For $N_f > 1$ the baryons correspond to instantons in the non-abelian D8-brane theory [11, 45]. This reproduces the known description of baryons as Skyrmions in the chiral Lagrangian. In this description the baryon charge comes from the CS term coupling the $U(1)_V$ field to the instanton density in the $SU(N_f)_V$ part.

able fluctuations corresponding to mesons, as one expects in a chiral-symmetric phase. Comparing the (Euclidean) actions of the two embeddings shows that the disconnected one becomes dominant when $T > 0.154/L$. In particular, for small L ($L < 0.97R_4$) the gauge theory has an intermediate phase of deconfinement with broken chiral symmetry.

22.3.2 Finite Density and Background Fields

The D8-brane worldvolume vector and axial gauge fields are dual to conserved vector and axial currents in the gauge theory, and therefore[5]

$$j^{\mu}_{V,A} = \frac{1}{\mathcal{N} V_4} \frac{\partial S_{D8}|_{on\text{-}shell}}{\partial a_{\mu}^{V,A}(u \to \infty)}. \tag{22.30}$$

The chemical potentials are defined by[6]

$$\mu_V = a_0^V(u \to \infty) \quad \text{and} \quad \mu_A = a_0^A(u \to \infty). \tag{22.31}$$

In our conventions quarks carry one unit of vector charge and baryons carry N_c units. Nevertheless we will refer to the vector current as the "baryon number current". We are also interested in studying the effects of background "electromagnetic" fields that couple to this current, which correspond to turning on spacetime dependent boundary values of the worldvolume gauge field, in particular

$$e_i = f_{0i}(u \to \infty), \qquad b_i = \varepsilon_{ijk} f_{jk}(u \to \infty). \tag{22.32}$$

In some situations one may be required to add boundary terms to the action. These are especially relevant if there is a CS term in the bulk. In deriving the equations of motion from the variational principle one usually assumes that the surface terms vanish. However in some instances one has to be more careful. The surface terms (in the $a_u = 0$ gauge) are given in general by

$$\delta S|_{on\text{-}shell} = \int d^4x \, \frac{\partial \mathscr{L}}{\partial a'_{\nu}} \delta a_{\nu} \Big|_{u_{min}}^{\infty} + \int d^3x \, du \, \frac{\partial \mathscr{L}}{\partial(\partial_{\mu} a_{\nu})} \delta a_{\nu} \Big|_{x_{\mu} \to -\infty}^{x_{\mu} \to \infty}. \tag{22.33}$$

In holography the boundary values of the fields at $u \to \infty$ are fixed, so $\delta a_{\mu}(u \to \infty) = 0$. However $\delta a_{\mu}(u_{min})$ and $\delta a_{\mu}(x_{\mu} \to \pm\infty)$ need not vanish. Therefore a sur-

[5]The axial symmetry is broken by an anomaly. However this is a subleading effect at large N_c which we can neglect. In particular, we will assume that the one-flavor pseudoscalar η' is massless. For a discussion of the $U(1)_A$ anomaly and the η' mass in the context of the Sakai-Sugimoto model see [11, 47].

[6]We would like to stress that this is a gauge invariant definition. The standard boundary condition on the gauge field in AdS/CFT fixes the value of $a_M(u \to \infty)$. In this case only the transformations that vanish at $u \to \infty$ are gauged in the bulk. In particular, these transformations do not change the asymptotic value of a_0.

face term may be non-trivial if the fields extend to these boundaries. In order to have a well-defined variational principle we must therefore add boundary terms $S_\partial(u_{min}) + S_\partial(x_\mu \to \pm\infty)$, whose variation cancels the surface terms in the variation of the bulk action.

These boundary terms also allow one to derive an alternative and useful definition of the conserved currents. We do this by varying the *off-shell* action, now allowing $a_\mu(u \to \infty)$ to vary, and then going on-shell by applying the equations of motion. Due to the boundary terms, only the surface term at $u \to \infty$ remains. Thus

$$j^\mu = \frac{1}{\mathcal{N}} \frac{\partial \mathcal{L}}{\partial a'_\mu}(u \to \infty)\Big|_{on\text{-}shell}. \tag{22.34}$$

In particular this relates the charge density in the boundary theory to the bulk radial electric field. The boundary term $S_\partial(u_{min})$ for a_0 should then be interpreted as a source term for this field. One could in principle also add boundary terms at $u \to \infty$. These have no effect on the derivation of the equations of motion, but may change the value of the on-shell action, and therefore may lead to additional contributions to (22.34).

A state with a non-zero baryon number density corresponds to an embedding with a radial electric field. In particular, for a U embedding (in both the confining and deconfining backgrounds) this requires the addition of a baryonic source at the tip, corresponding to a uniform spatial distribution of wrapped D4-branes (Figs. 22.6d, 22.6e) [48] (see also [49, 50]). We assume that the distribution is dilute enough so that we can ignore interactions between the D4-branes. We should therefore include the D4-brane action, which is given by (in the confining background)

$$S_{D4} = -\mathcal{N} V_4 n_{D4} N_c \left(\frac{1}{3}u_0 - a_0^V(u_0)\right), \tag{22.35}$$

where n_{D4} is the density of D4-branes. The first term is the D4-brane DBI action, and corresponds to the baryon mass, and the second term comes from the N_c strings that connect each D4-brane to the D8-brane. The second term is precisely the boundary term at $u_{min} = u_0$ that was discussed above.

The resulting asymptotic behavior of the gauge field is

$$a_0^V(u) \approx \mu_V - \frac{2}{3}\frac{d}{u^{3/2}}, \tag{22.36}$$

where $d = N_c n_{D4}$ is the baryon number density. On the other hand, extremizing the action with respect to n_{D4} fixes the value of the gauge field at the tip to $a_0^V(u_0) = u_0/3 = m_{baryon}/N_c$. This implies, as expected, that a non-zero density configuration exists only when the chemical potential is above the baryon mass. In fact the non-zero density state is always the dominant one. The transition to "nuclear matter" occurs at $\mu_V = m_{baryon}/N_c$. Near the critical point the density scales linearly with the chemical potential $d \sim \mu_V - m_{baryon}/N_c$. The D4-brane action also sources the embedding field $x_4(u)$, creating a cusp at $u = u_0$. This can be understood in terms

of a force balance condition between the D4-branes pulling down and the D8-brane pulling up.

At high temperature the preferred embedding is parallel and there is a different finite density solution. In this case the gauge fields a_μ and $\bar{a}_\mu$ are independent, and the field theory has a conserved axial current as well as a baryon current. For a baryonic solution we take $a_0^V(\infty) = \mu_V$ and $a_0^A(\infty) = 0$. In addition, since the D8-brane and anti-D8-brane reach the horizon we must impose $a_0^V(u_T) = a_0^A(u_T) = 0$. Therefore the radial vector electric field, and thus the baryon number density, is non-zero when $\mu_V > 0$. In this phase $d \sim T^3 \mu_V$ for small μ_V.

22.3.3 Magnetic Catalysis of Chiral Symmetry Breaking

A strong magnetic field in QCD is believed to catalyze the spontaneous breaking of chiral symmetry [1–3]. The basic mechanism for this is that in a strong magnetic field all the quarks sit in the lowest Landau level, and the dynamics is effectively $1+1$-dimensional. This phenomenon has been exhibited in the Sakai-Sugimoto model in [51, 52].[7]

With a uniform background magnetic field b, the D8-brane action in the deconfining background becomes

$$S_{D8}^{dec} = -\mathcal{N} \int d^4x\, du\, u^4 \sqrt{\left(f(u)\left(x_4'(u)\right)^2 + \frac{1}{u^3}\right)\left(1 + \frac{b^2}{u^3}\right)}. \qquad (22.37)$$

The U embedding has the same form as before (22.26), but now u_0 depends on the magnetic field, as shown in Fig. 22.7a. The mass scale associated with chiral symmetry breaking is seen to increase with the magnetic field. One therefore expects that chiral symmetry breaking becomes more favored as the magnetic field increases. This is indeed the case, as can be seen by comparing the Euclidean actions of the U and parallel embeddings as the temperature and magnetic field are varied. The resulting phase diagram is shown in Fig. 22.7b. We observe that in this model the critical temperature approaches a finite value at infinite magnetic field.

A qualitatively similar effect was observed in the D3–D7 model above. However in the D3–D7 model there is a critical value of B/T^2 above which the chiral symmetry is always broken, whereas in the D4–D8 there is a critical temperature above which the chiral symmetry is always broken.

It is also instructive to study the effect of the background magnetic field on the mesons. This was partly done in [55], in which the high spin mesons were studied. It was shown that the magnetic field enhances their stability by increasing their angular momentum, and thereby increasing the dissociation temperature at which they fall apart into their quark constituents. This is consistent with the above results.

[7] At non-zero baryon number density the magnetic field can actually induce an inverse magnetic catalysis in this model [53, 54].

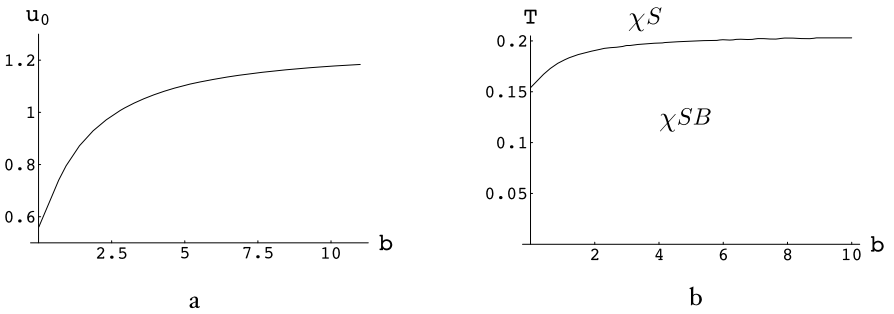

Fig. 22.7 Magnetic catalysis: **(a)** Chiral symmetry breaking mass scale. **(b)** Phase diagram

22.3.4 Anomalous Currents

The chiral anomaly leads to two interesting phenomena when both the magnetic field and chemical potential are non-zero. The first is the generation of anomalous currents in the chiral symmetric phase of QCD. In [56, 57] it was shown that the combination of a magnetic field and a non-zero baryon chemical potential generates an axial current

$$\mathbf{J}_A = \frac{e}{2\pi^2}\mu_B^{phys}\mathbf{B}. \tag{22.38}$$

Since the source for this current is the anomaly it is an exact result, and should be valid in particular at strong coupling. Similarly, an anomalous vector current is generated in a non-zero axial chemical potential:

$$\mathbf{J}_V = \frac{e}{2\pi^2}\mu_A^{phys}\mathbf{B}. \tag{22.39}$$

This is known as the "chiral magnetic effect", and may have some relevance to heavy ion physics at RHIC [5]. Within the D3/D7 model, this effect has been discussed in [58].

In the Sakai-Sugimoto model, the chiral-symmetric phase corresponds to the parallel D8–$\overline{\text{D8}}$ embedding in the deconfined background, and the chiral anomaly is encoded in the five-dimensional CS term (22.24). The background magnetic field and chemical potentials correspond to different components of the worldvolume gauge field. Through the five-dimensional CS term these source a third component, which corresponds to a current in the four-dimensional theory [59]. Let us review the calculation of the anomalous axial current in the Sakai-Sugimoto model. The calculation of the anomalous vector current is virtually identical.

To be specific, we will consider a background magnetic field in the x_1 direction by turning on a background gauge field $a_3^V = x_2 b$. A non-trivial boundary value of a_0^V will then source, via the CS term, a non-trivial a_1^A. In general a_0^V and a_1^A can depend on both u and x_2 in this case, although on-shell they will depend only on u. We will take $a_0^V(\infty) = \mu_V$ and $a_1^A(\infty) = 0$. The D8-brane DBI and CS actions in

this case become

$$S_{DBI}^{dec} = -\mathcal{N}\int_{u_T}^{\infty} d^4x\, du\, u^{5/2}\sqrt{\left(1-\left(a_0^{V\prime}\right)^2+f(u)\left(a_1^{A\prime}\right)^2\right)\left(1+\frac{b^2}{u^3}\right)}, \tag{22.40}$$

$$S_{CS} = -\mathcal{N}\int d^4x\, du\left[b\left(a_0^V a_1^{A\prime}-a_0^{V\prime}a_1^A\right)+a_3^V\left(a_0^{V\prime}\partial_2 a_1^A-\partial_2 a_0^V a_1^{A\prime}\right)\right]. \tag{22.41}$$

The necessary boundary terms are

$$S_\partial = -\frac{1}{2}\mathcal{N}\int d^3x\, du\, a_3^V\left(a_0^V a_1^{A\prime}-a_0^{V\prime}a_1^A\right)\Big|_{x_2\to-\infty}^{x_2\to\infty}. \tag{22.42}$$

By integrating by parts the last two terms in the CS action one can show that up to a surface term at $u\to\infty$, the bulk CS and boundary actions combine into a bulk action

$$\begin{aligned} &S_{CS}+S_\partial \\ &\quad = -\mathcal{N}\int d^4x\, du\left[\frac{3}{2}b\left(a_0^V a_1^{A\prime}-a_0^{V\prime}a_1^A\right)-\frac{1}{2}a_3^{V\prime}\left(a_0^V\partial_2 a_1^A-\partial_2 a_0^V a_1^A\right)\right]. \end{aligned} \tag{22.43}$$

One can get rid of the remaining surface term by adding a boundary term at $u\to\infty$ [59], however this particular term does not contribute to the on-shell action, so we might as well ignore it.[8]

The equations of motion for $a_0^V(u)$ and $a_1^A(u)$ can be integrated once to yield

$$\frac{\sqrt{u^5+b^2u^2}\,a_0^{V\prime}(u)}{\sqrt{1-(a_0^{V\prime}(u))^2+f(u)(a_1^{A\prime}(u))^2}} = -3ba_1^A(u)+d, \tag{22.44}$$

$$\frac{\sqrt{u^5+b^2u^2}\,f(u)a_1^{A\prime}(u)}{\sqrt{1-(a_0^{V\prime}(u))^2+f(u)(a_1^{A\prime}(u))^2}} = -3ba_0^V(u), \tag{22.45}$$

where d is the baryon number charge density. The integration constant in the a_1^A equation vanishes since $a_0^V(u_T)=0$ and $f(u_T)=0$. Using (22.34) and (22.45) we can then evaluate the axial current:

$$j_A^1 = \frac{3}{2}ba_0^V(\infty) = \frac{3}{2}b\mu_V. \tag{22.46}$$

The correctly normalized physical currents are given by $J=2(2\pi\alpha'\mathcal{N}/R^5)j$, where the factor of 2 comes from adding the anti-D8-brane contribution, and the physical chemical potentials are $\mu^{phys}=(R/(2\pi\alpha'))\mu$. Thus in terms of the physical variables our result translates to

[8] Other boundary terms at $u\to\infty$ could affect the on-shell action, and therefore the currents. See for example [60, 61].

$$\mathbf{J}_A = \frac{N_c}{4\pi^2}\mu_V^{phys}\mathbf{B}. \tag{22.47}$$

Similarly, for an axial chemical potential we would get

$$\mathbf{J}_V = \frac{N_c}{4\pi^2}\mu_A^{phys}\mathbf{B}. \tag{22.48}$$

Interestingly, our results are half of the weak-coupling results (where $e = N_c$ in the holographic model). It has been argued that the discrepancy in the axial current is due to a different treatment of the triangle anomaly, consistent vs. covariant, and can be corrected by adding an appropriate Bardeen counterterm on the boundary [61]. However, the same counterterm leads to a vanishing vector current. This issue is still under investigation.

22.3.5 The Pion Gradient Phase

In the broken chiral symmetry phase the chiral anomaly leads to a novel finite density phase that dominates over nuclear matter at large magnetic fields [4]. In this phase the baryon charge is carried not by baryons but rather by a non-zero pion gradient background:

$$D = \frac{e}{4\pi^2 f_\pi}\mathbf{B}\cdot\nabla\pi^0, \tag{22.49}$$

where

$$\nabla\pi^0 = \frac{e}{4\pi^2 f_\pi}\mu_B^{phys}\mathbf{B}. \tag{22.50}$$

In the Sakai-Sugimoto model (in the $a_u = 0$ gauge) the pseudoscalar meson appears in the zero mode of a_μ^A (22.27), so

$$\partial_\mu\varphi\left(x^\mu\right) = -a_\mu^A\left(x^\mu, u\to\infty\right). \tag{22.51}$$

As in the chiral-symmetric phase, the presence of a vector chemical potential together with a background magnetic field sources a component of the axial gauge field, which in this case corresponds to a non-trivial gradient of the pseudoscalar field [59, 62]. Since there is only one flavor this field should really be thought as the η' meson. For simplicity, we will consider only the confined phase with the antipodal D8-brane embedding, namely $u_0 = u_{KK}$. (The results do not change qualitatively for more general U-shape embeddings, or for U-shape embeddings in the deconfined phase.)

Following [59], the D8-brane DBI action in this case is

$$S_{DBI}^{con} = -\mathscr{N}\int_{u_{KK}}^{\infty} d^4x\, du\, u^{5/2}\sqrt{\left(\frac{1}{f(u)} - \left(a_0^{V\prime}\right)^2 + \left(a_1^{A\prime}\right)^2\right)\left(1+\frac{b^2}{u^3}\right)}, \tag{22.52}$$

and the CS plus boundary actions are the same as in the deconfined phase (22.43). The equations of motion integrate to

$$\frac{\sqrt{u^5+b^2u^2}a_0^{V\prime}(u)}{\sqrt{\frac{1}{f(u)}-(a_0^{V\prime}(u))^2+(a_1^{A\prime}(u))^2}}=-3ba_1^A(u)+N_c\,n_{D4}, \tag{22.53}$$

$$\frac{\sqrt{u^5+b^2u^2}a_1^{A\prime}(u)}{\sqrt{\frac{1}{f(u)}-(a_0^{V\prime}(u))^2+(a_1^{A\prime}(u))^2}}=-3ba_0^V(u)+c, \tag{22.54}$$

where we have explicitly included the baryon sources in the a_0^V equation. Our boundary conditions are now $a_0^V(\infty)=\mu_V$ and $a_1^A(\infty)=-\nabla\varphi(x^\mu)$. In particular $a_1^A(\infty)$ is a field rather than a parameter in the boundary theory, and we must minimize the action with respect to its value. This simply sets $j_A^1=0$ and therefore sets the integration constant in the a_1^A equation to $c=\frac{3}{2}b\mu_V$.[9]

We can now compute the total baryon number charge density d using the same procedure as in the previous section for the current. In the absence of sources $n_{D4}=0$ and we find

$$d=-\frac{3}{2}ba_1^A(\infty)=\frac{3}{2}b\nabla\varphi. \tag{22.55}$$

Let us express this in terms of the physical variables. First we must define a field with a canonically normalized kinetic term. Inserting (22.27) into the action (22.52) we find that the canonically normalized field is given by

$$\eta'\big(x^\mu\big)=\frac{R^2}{2\pi\alpha'}f_{\eta'}\varphi\big(x^\mu\big),\qquad f_{\eta'}^2=\frac{N_c\,u_{KK}^{3/2}}{4\pi^4\alpha'}. \tag{22.56}$$

Converting to physical variables we then find

$$D=\frac{N_c}{4\pi^2 f_{\eta'}}\mathbf{B}\cdot\boldsymbol{\nabla}\eta', \tag{22.57}$$

in agreement with (22.49). We would like to stress that this agreement did not depend on the specific value of $f_{\eta'}$ required for canonical normalization, since it cancels out when we express the result in terms of φ. The correct numerical factor of $1/(4\pi^2)$ is a direct consequence of including the proper boundary terms in the action, leading to the "3/2" in (22.55).

To find the value of the gradient $\nabla\varphi$ we need to solve (22.53) and (22.54). The result will not be as simple as (22.50). In particular it is not linear in the magnetic field, since we are using the full non-linear DBI action. It turns out that a closed form solution can be found in terms of a new variable

[9] This is also consistent with the fact that there are no quarks in this phase to carry such a current.

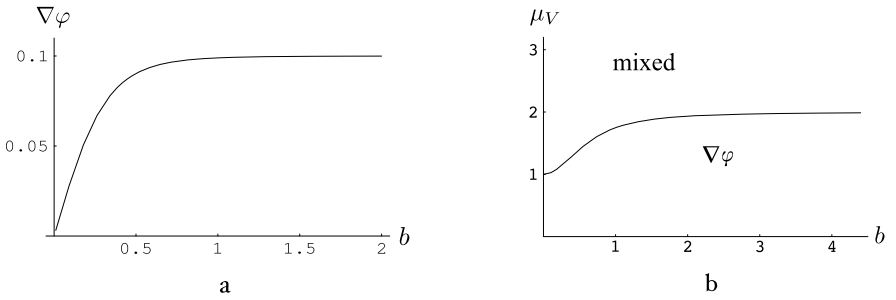

Fig. 22.8 **(a)** The pion gradient. **(b)** Phase diagram with magnetic field and baryon chemical potential

$$y = \int_{u_{KK}}^{u} \frac{3b\, d\tilde{u}}{\sqrt{f(\tilde{u})}\sqrt{\tilde{u}^5(1+b^2\,\tilde{u}^{-3}) - (\frac{3}{2}b\mu_V)^2 + (3b\nabla\varphi)^2}}. \tag{22.58}$$

The solution is

$$a_0^V(y) = \frac{\mu_V}{2}\left(\frac{\cosh y}{\cosh y_\infty} + 1\right), \qquad a_1^A(y) = -\frac{\mu_V}{2}\frac{\sinh y}{\cosh y_\infty}, \tag{22.59}$$

where $y_\infty = y(u \to \infty)$. The pseudoscalar gradient is then given by

$$\nabla\varphi = -a_1^A(\infty) = \frac{\mu_V}{2}\tanh y_\infty. \tag{22.60}$$

The dependence on b is shown in Fig. 22.8a. For small b the behavior is linear in b:

$$\nabla\varphi \approx \frac{\pi}{2u_{KK}^{3/2}}\mu_V b, \tag{22.61}$$

and in terms of the physical quantities:

$$\boldsymbol{\nabla}\eta' \approx \frac{N_c}{4\pi^2 f_{\eta'}}\mu_V^{phys}\mathbf{B}, \tag{22.62}$$

in agreement with the single flavor version of (22.50).

As in the case with no magnetic field, an embedding that includes sources is possible above a critical value of the chemical potential, which then becomes the dominant configuration. This describes a "mixed phase" that includes both "pion-gradient" matter and nuclear matter, with a total baryon number density

$$d = \frac{3}{2}b\nabla\varphi + N_c\, n_{D4}. \tag{22.63}$$

As before, one can find a closed form solution for a_0^V and a_1^A, and from it determine the values of $\nabla\varphi$ and n_{D4} in terms of the magnetic field b and baryon num-

ber chemical potential μ_V. The resulting phase diagram is shown in Fig. 22.8b. In particular, the critical value of μ_V is determined by setting $n_{D4} = 0$. The relative proportion of baryons in the mixed phase increases with μ_V and decreases with b.

22.3.6 Magnetic Phase Transition

The high-temperature chiral-symmetric phase of this model also exhibits an interesting magnetic phenomenon associated with the distribution of the baryonic charge [63]. In what follows we analyze the situation for the D8-brane. As in the broken chiral symmetry phase above, the distribution of baryonic charge along the radial direction u changes with b. We can therefore identify two types of baryonic charge, one originating from the horizon, and the other from outside the horizon. The latter d_*, corresponds to D4-branes that are radially smeared inside the D8-brane. This can be best seen from the longitudinal and transverse conductivities [64]

$$\sigma_L = \frac{\sqrt{u_T^8 + b^2 u_T^5 + u_T^3 (d - d_*)^2}}{u_T^3 + b^2}, \tag{22.64}$$

$$\sigma_T = \frac{b(d - d_*)}{u_T^3 + b^2} + \frac{d_*}{b}, \tag{22.65}$$

where $d_* = -3ba_1(u_T)$. In particular only the horizon charge $d - d_*$ contributes to the longitudinal conductivity. In the transverse conductivity, the horizon charge contributes as an ordinary dissipative fluid, whereas the charge outside the horizon d_* behaves as a dissipation-free fluid. This is consistent with an interpretation of d_* as the charge filling the lowest Landau level. As the magnetic field increases more of the charge is "lifted" from the horizon, representing the transition to the lowest Landau level in the boundary theory.

In fact for a fixed density at low enough temperature this transition is a first order phase transition as a function of the magnetic field, in which the charges jump into the lowest Landau level. This is easiest to see in the zero temperature limit.[10] In this case one can solve the gauge field equations analytically in terms of a variable

$$z = \int_0^u \frac{3b\, d\tilde{u}}{\sqrt{\tilde{u}^5 + b^2 \tilde{u}^2 + d^2 \cosh^{-2} z_\infty}}, \tag{22.66}$$

where $z_\infty = z(u \to \infty)$. The solution is

[10] Strictly speaking, at zero temperature the theory is in the confining (and broken chiral symmetry) phase. We are considering the meta-stable state obtained by adiabatically reducing the temperature.

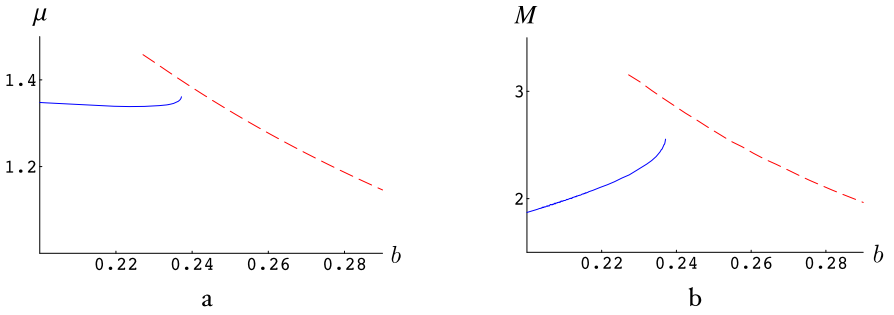

Fig. 22.9 **(a)** μ and **(b)** M as functions of b for $d = 1$ and $T = 0.09$, below the critical point. There are now two branches of stable solutions, and the phase transition between them occurs at $b = 0.235$

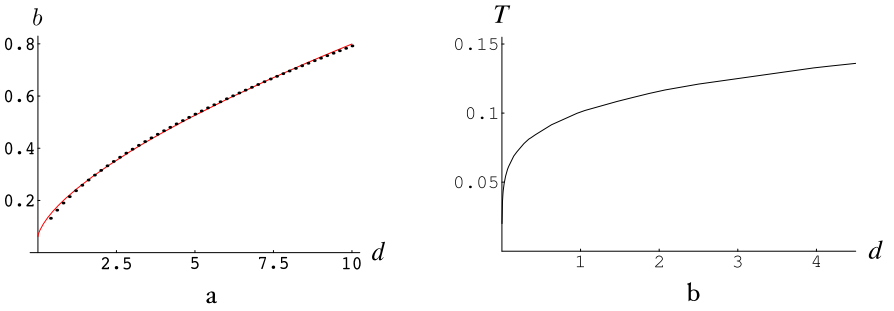

Fig. 22.10 **(a)** The phase diagram in the d–b plane at $T = 0.07$, and **(b)** the critical line in the T–d plane

$$a_0^V = \frac{d \sinh z}{3b \cosh z_\infty}, \qquad a_1^A = \frac{d \cosh z}{3b \cosh z_\infty} - \frac{d}{3b}. \tag{22.67}$$

There are actually three solutions, representing two stable phases and an unstable phase. As the magnetic field b is increased, for a fixed total baryon number density d, one finds a first order phase transition between the two stable phases. Both the magnetization and the chemical potential are discontinuous in this transition (Fig. 22.9), which is reminiscent of a metamagnetic phase transition. The large magnetic field phase represents the situation where all the charge is in the lowest Landau level, with the chemical potential and free energy given by

$$\mu = \frac{d}{3b}, \qquad F = \frac{d^2}{6b}. \tag{22.68}$$

The magnetic transition persists also at non-zero temperatures that are low relative to the density d. Too a very good approximation this happens when $b \sim d^{2/3}$ (Fig. 22.10a), which is the behavior expected for the lowest Landau level. At high temperature the transition disappears (Fig. 22.10b).

22.4 The D3–D7' Model

The study of magnetic properties of planar matter is a very active area of research in condensed matter physics. A simple holographic model for charged fermions in three dimensions can be obtained by T-dualizing the D4–D8 setup. This leads to a D3–D7 configuration with the two sets of branes intersecting on a plane [12, 14] (for a related model using a D2–D8 system see [65]). However, unlike in the D4–D8 configuration, here the branes have a mutually transverse coordinate. On the one hand this allows the fermions to be massive, but on the other hand it leads to an instability since the different branes repel.

22.4.1 Stable Embeddings

First we have to address the issue of stability. As before, we will employ the probe approximation and consider a single probe D7-brane. The background (at finite temperature) in this case is

$$L^{-2}\,ds_{10}^2 = r^2\big(-h(r)\,dt^2 + dx^2 + dy^2 + dz^2\big) + r^{-2}\left(\frac{dr^2}{h(r)} + r^2\,d\Omega_5^2\right), \quad (22.69)$$

$$F_5 = 4L^4\big(r^3\,dt\wedge dx\wedge dy\wedge dz\wedge dr + d\Omega_5\big), \quad (22.70)$$

where $h(r) = 1 - r_T^4/r^4$, $r_T = \pi LT$ and $L^2 = \sqrt{4\pi g_s N_c}\alpha'$. It is convenient to parameterize the five-sphere as an $S^2 \times S^2$ fibered over an interval:

$$d\Omega_5^2 = d\psi^2 + \cos^2\psi\big(d\Omega_2^{(1)}\big)^2 + \sin^2\psi\big(d\Omega_2^{(2)}\big)^2, \quad (22.71)$$

where $0 \le \psi \le \pi/2$. The first S^2 shrinks at the "south pole" $\psi = \pi/2$ and the second S^2 at the "north pole" $\psi = 0$. The D7-brane wraps the two S^2's and extends along (x, y), and has an embedding described by $z(r)$ and $\psi(r)$. In particular ψ is dual to the fermion bi-linear operator in the field theory corresponding to the fermion mass. The D7-brane DBI action in this background is given by

$$S_{DBI} = -4\mathcal{N}\int d^3x\,dr\,r^2\cos^2\psi\sin^2\psi\sqrt{1 + r^4h(r)z'^2 + r^2h(r)\psi'^2}, \quad (22.72)$$

where $\mathcal{N} \equiv 4\pi^2\mu_7 L^8/g_s$. A massless embedding would correspond to $\psi = \pi/4$. However the fluctuations contain a mode that violates the Breitenlohner-Freedman bound, and therefore the embedding is unstable. This can also be seen by trying a more general embedding with a large r behavior of

$$\psi(r) \sim \frac{\pi}{4} + cr^{\Delta}. \quad (22.73)$$

The equation of motion for ψ gives $\Delta(\Delta + 3) = -8$, which does not have a real solution.

Fortunately, the D7-brane can be stabilized by turning on some worldvolume flux [66], in this case on the two-spheres [15]:

$$2\pi\alpha' F = \frac{L^2}{2}\left(f_1\, d\Omega_2^{(1)} + f_2\, d\Omega_2^{(2)}\right), \quad f_i = \frac{2\pi\alpha'}{L^2} n_i \quad (n_i \in \mathbb{Z}). \tag{22.74}$$

This changes the DBI action,

$$S_{DBI} = -\mathcal{N}\int d^3x\, dr\, r^2 \sqrt{\left(4\cos^4\psi + f_1^2\right)\left(4\sin^4\psi + f_2^2\right)\left(1 + r^4 h z'^2 + r^2 h \psi'^2\right)}, \tag{22.75}$$

and there is now also a CS term which gives,

$$S_{CS} = -\mathcal{N} f_1 f_2 \int d^3x\, dr\, r^4 z'(r). \tag{22.76}$$

The asymptotic behavior of $\psi(r)$ is now

$$\psi(r) \sim \psi_\infty + m r^{\Delta_+} - c_\psi r^{\Delta_-}, \tag{22.77}$$

where ψ_∞ is determined by the solution of

$$\left(f_1^2 + 4\cos^4\psi_\infty\right)\sin^2\psi_\infty = \left(f_2^2 + 4\sin^4\psi_\infty\right)\cos^2\psi_\infty, \tag{22.78}$$

and

$$\Delta_\pm = -\frac{3}{2} \pm \frac{1}{2}\sqrt{9 + 16\frac{f_1^2 + 16\cos^6\psi_\infty - 12\cos^4\psi_\infty}{f_1^2 + 4\cos^6\psi_\infty}}\,. \tag{22.79}$$

In particular, the embedding is stable for a large enough flux. The coefficient of the leading term is related to the fermion mass, and that of the subleading term corresponds to the bi-linear condensate. Note that the scaling dimension of the bi-linear operator is given by $-\Delta_-$. This represents a large anomalous dimension, which is not surprising given that the model is non-supersymmetric. We should require however that the operator be relevant, namely that $\Delta_- \geq -3$, and therefore that $\Delta_+ \leq 0$, in order to consider the leading term as a "mass deformation".

Generally there are two types of embeddings, that differ in their small r behavior: Minkowski-like (MN) embeddings, in which the D7-brane terminates smoothly outside the horizon (Fig. 22.11a), and black-hole (BH) embeddings, in which the D7-brane crosses the horizon (Fig. 22.11b). We refer the reader to [15] for the explicit embedding equations for $\psi(r)$ and $z(r)$, and for their numerical solutions.

In an MN embedding $\psi(r_0) = \pi/2$ or 0 for some $r_0 > r_T$, corresponding to one or the other S^2 shrinking. This indicates that the dual field theory has a mass-gap related to $r_0 - r_T$. An important condition for the existence of MN embeddings is the absence of sources for the worldvolume gauge field. Unlike in the model

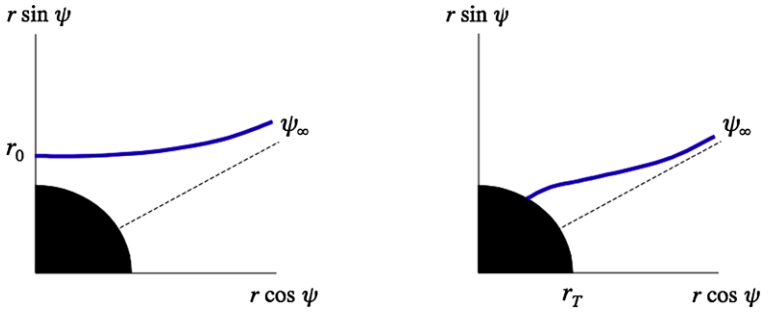

Fig. 22.11 **(a)** An MN embedding with $\psi(r_0) = \pi/2$. **(b)** A BH embedding

of the previous section, there are no localized sources in this model. All sources correspond to branes (or strings) connecting the D7-brane to the horizon. These inevitably pull the D7-brane down to the horizon, resulting in a BH embedding instead. This means that the flux on the S^2 that shrinks must vanish. For $\psi(r_0) = \pi/2$, which means that $f_1 = 0$, we find stable massive embeddings in the range

$$0.5235 \lesssim \psi_\infty \lesssim 0.6251. \tag{22.80}$$

(There are also the "mirror" embeddings with $\psi(r_0) = 0$ and $f_2 = 0$.) Note that the allowed values of ψ_∞ are quantized since the stabilizing flux is quantized. There are also two isolated MN embeddings with $\psi_\infty = 0$ and $\psi_\infty = \pi/2$.

BH embeddings describe gapless phases in the dual theory. These embeddings exist generically for any f_1, f_2 satisfying the stability condition.

22.4.2 Finite Density and Background Fields

For embeddings corresponding to finite density states in a background magnetic field we need to turn on the appropriate components of the worldvolume gauge field. As in the D4–D8 model we will work with the dimensionless field $a_\mu = (2\pi\alpha'/L)A_\mu$. There are additional terms in the DBI action,

$$S_{DBI} = -\mathcal{N}\int dr\, r^2 \sqrt{\left(4\cos^4\psi + f_1^2\right)\left(4\sin^4\psi + f_2^2\right)} \times \sqrt{\left(1 + r^4 h(r) z'^2 + r^2 h(r)\psi'^2 - a_0'^2\right)\left(1 + \frac{b^2}{r^4}\right)}, \tag{22.81}$$

and also in the CS action,

$$S_{CS} = -\mathcal{N} f_1 f_2 \int dr\, r^4 z'(r) + 2\mathcal{N}\int dr\, c(r) b a_0'(r), \tag{22.82}$$

where

$$c(r) = \frac{1}{8\pi^2 L^4}\int_{S^2\times S^2} C_4\big(\psi(r)\big) = \psi(r) - \frac{1}{4}\sin 4\psi(r) - \psi_\infty + \frac{1}{4}\sin 4\psi_\infty. \tag{22.83}$$

We have fixed a gauge for the RR field such that $c(\infty) = 0$. For MN embeddings we must also add a boundary term at $r = r_0$ (as explained in Sect. 22.3)[11]

$$S_\partial(r_0) = 2\mathscr{N} c(r_0) b a_0(r_0). \tag{22.84}$$

The quantity $c(r_0)$ has a nice physical interpretation: it is the total amount of 5-form flux captured by the D7-brane in the MN embedding. It is completely fixed by the asymptotic value of the embedding angle ψ_∞. For BH embeddings the boundary term vanishes since $a_0(r_T) = 0$.

The integrated equation of motion for $a_0(r)$ is given by

$$G(r)a_0'(r) = d - 2bc(r), \tag{22.85}$$

where

$$G(r) = r^2\left(1+\frac{b^2}{r^4}\right)\sqrt{\frac{(f_1^2+4\cos^4\psi)(f_2^2+4\sin^4\psi)}{Y(r)}}, \tag{22.86}$$

$$Y(r) = \left(1+\frac{b^2}{r^4}\right)\left(1+hr^4z'^2+hr^2\psi'^2-a_0'^2\right), \tag{22.87}$$

and d is the total charge density. As in Sect. 22.3, we are using (22.34) to define the conserved currents. The quantity on the RHS of (22.85), $\tilde{d}(r) \equiv d - 2bc(r)$, is the contribution to the charge density from radial positions below r.

We would also like to study the response of the system to a background electric field. To this end we should consider a more general ansatz for the gauge field with $a_x(t,r) = te + a_x(r)$, $a_y(x,r) = xb + a_y(r)$, in addition to $a_0(r)$. The current densities will be contained in the asymptotic behaviors of $a_x(r)$ and $a_y(r)$. The gauge field equations in this case become

$$G(r)\,a_0'(r) = \left[\tilde{d}(r)\left(1-\frac{e^2}{r^4h(r)}\right)+\tilde{j}_y(r)\frac{eb}{r^4h(r)}\right]\frac{1+\frac{b^2}{r^4}}{1+\frac{b^2}{r^4}-\frac{e^2}{r^4h(r)}}, \tag{22.88}$$

$$G(r)\,a_y'(r) = \left[\tilde{d}(r)\frac{eb}{r^4h(r)}-\frac{\tilde{j}_y(r)}{h(r)}\left(1+\frac{b^2}{r^4}\right)\right]\frac{1+\frac{b^2}{r^4}}{1+\frac{b^2}{r^4}-\frac{e^2}{r^4h(r)}}, \tag{22.89}$$

[11] In [15] this term was derived by demanding invariance of the CS term $\int C_4\wedge F\wedge F$ under gauge transformations of the RR field and then fixing $c(\infty)=0$. However it can also be obtained by canceling the surface term in the variation of the CS term, when we present it as $\int F_5\wedge A\wedge F$.

$$G(r)\,a_x'(r) = -\frac{j_x}{h(r)}\left(1+\frac{b^2}{r^4}\right), \tag{22.90}$$

where j_x is the longitudinal current density and $\tilde{j}_y(r)$ is defined by analogy with $\tilde{d}(r)$ as $\tilde{j}_y(r) \equiv j_y - 2c(r)e$, where j_y is the transverse current density. The factor $G(r)$ is defined as before (22.86), now more generally with

$$\begin{aligned} Y(r) = &\left(1+\frac{b^2}{r^4}-\frac{e^2}{hr^4}\right)\left(1+hr^4z'^2+hr^2\psi'^2\right) \\ &-\left(1+\frac{b^2}{r^4}\right)a_0'^2+ha_x'^2+\left(1-\frac{e^2}{hr^4}\right)ha_y'^2-\frac{2eb}{r^4}a_0'a_y'. \end{aligned} \tag{22.91}$$

22.4.3 Quantum Hall States

Let us consider first the response of the gapped MN embeddings. This is determined by the requirement that there are no sources, namely by regularity of the gauge field at $r = r_0$. This implies, in particular, that

$$\tilde{d}(r_0) = d - 2c(r_0)b = 0. \tag{22.92}$$

The entire charge in the MN embedding is thus due to the CS term and corresponds to a "fluid" of D5-branes inside the D7-brane. The charge density is proportional to the magnetic field, and the proportionality constant is fixed by the value of $c(r_0)$, and therefore of ψ_∞. This is the key property of a quantum Hall state, which is characterized by a specific quantized value of the Landau-level filling fraction $\nu \propto d/b$. In terms of the physical variables $D = (2\pi\alpha'\mathcal{N}/L^4)d$ and $B = b/(2\pi\alpha')$, the filling fraction is given by

$$\nu = \frac{2\pi D}{B} = \frac{2N_c}{\pi}c(r_0). \tag{22.93}$$

For the range of values of ψ_∞ needed for stability (22.80) we get

$$0.6972 \lesssim \frac{\nu}{N_c} \lesssim 0.8045. \tag{22.94}$$

Furthermore, the filling fractions are quantized according to the quantization of ψ_∞. The actual numbers can be obtained by solving (22.78), for a specific flux f_2 (with $f_1 = 0$), and plugging into (22.83) with $\psi(r_0) = \pi/2$, but they are not particularly illuminating (for example, they are not rational numbers). The isolated embeddings with $\psi_\infty = 0$ and $\psi_\infty = \pi/2$ correspond to $\nu/N_c = 1$ and 0, respectively.

The current densities can likewise be computed by requiring regularity of the spatial components of the gauge field. This condition implies that

$$j_x = 0 \quad \text{and} \quad \tilde{j}_y(r_0) = j_y - 2c(r_0)e = 0, \tag{22.95}$$

from which we can deduce the longitudinal and transverse conductivities:

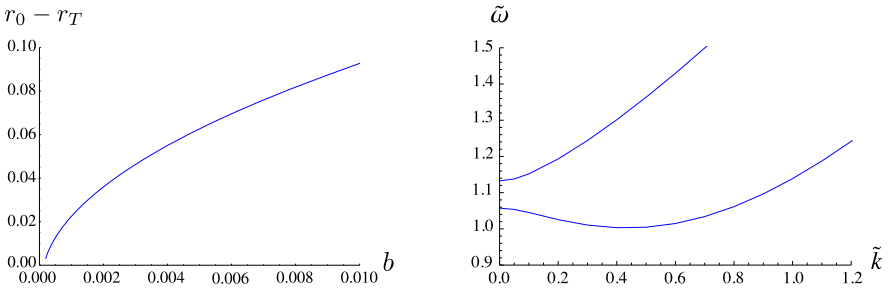

Fig. 22.12 **(a)** Mass-gap for charged states as a function of the magnetic field. **(b)** Dispersion relation of the two lowest neutral modes, showing the magneto-roton

$$\sigma_{xx} = 0, \qquad \sigma_{xy} = \frac{\nu}{2\pi}. \tag{22.96}$$

Thus the MN embeddings, when they exist, describe quantum Hall states with quantized transverse conductivities, and vanishing longitudinal conductivities. Furthermore, in the holographic description, the quantization is topological since it originates from the Dirac quantization of the magnetic fluxes on the S^2's. In particular, σ_{xy} in the MN embeddings is independent of the temperature.

Quantum Hall states are gapped to both charged and neutral excitations. In this model charged excitations are described by strings stretched from the D7-brane to the horizon, and therefore have a mass proportional to $r_0 - r_T$. This is seen to increase with the magnetic field, as shown in Fig. 22.12a. The neutral excitations correspond to fluctuations of the D7-brane worldvolume fields, and are also found to be massive [67] (see also [68]). The spectrum of neutral excitations includes a magneto-roton, which is a collective excitation whose dispersion relation has a minimum at non-zero momentum (Fig. 22.12b). A similar phenomenon is seen in real quantum Hall states [69].

22.4.4 Fermi-Like Liquid

BH embeddings describe gapless Fermi-like liquids. For a BH embedding, $\tilde{d}(r_T)$ corresponds to the horizon charge density carried by the "quarks", and it need not vanish. In particular, if we add sources to an MN embedding, thereby violating (22.92), it deforms continuously into a BH embedding with horizon charge.

To compute the electrical response in a BH embedding we have a couple of options. The standard approach is to extract the conductivities using linear response from the current-current correlators, computed holographically by studying fluctuations of the bulk gauge fields to quadratic order. The other option is to find a consistent solution in the presence of an external electric field [70]. The advantage of the second approach, when it is applicable, is that it gives the complete non-linear response. Using this method for the BH embeddings one finds

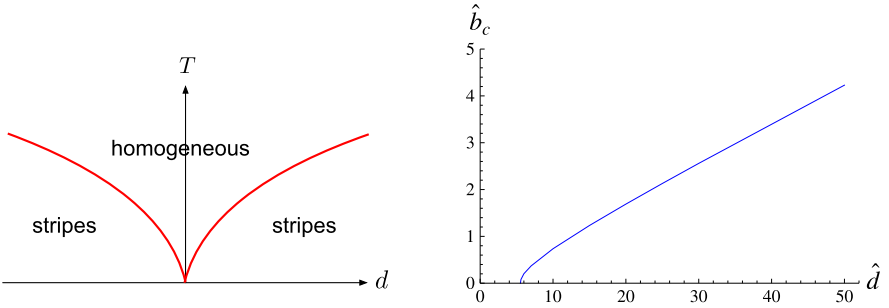

Fig. 22.13 (*Left*): Phase diagram in the T–d plane showing the quantum critical point. (*Right*): The phase diagram in the $\hat{b}, \hat{d}$ plane for $m = 0$. *Above the line* the system is in the homogeneous phase and *below the line* in the striped phase

$$\sigma_{xy} = \frac{N_c}{2\pi^2}\left(\frac{b}{b^2 + r_T^4}\tilde{d}(r_T) + 2c(r_T)\right), \tag{22.97}$$

$$\sigma_{xx} = \frac{N_c}{2\pi^2}\frac{r_T^2}{b^2 + r_T^4}\sqrt{\tilde{d}(r_T)^2 + \left(f_1^2 + 4\cos^4\psi(r_T)\right)\left(f_2^2 + 4\sin^4\psi(r_T)\right)\left(b^2 + r_T^4\right)}. \tag{22.98}$$

Note that the transverse conductivity has two components. The first involves the horizon charge, and resembles the contribution of an ordinary dissipative system of charges. The remaining charge, corresponding to the fluid of D5-branes inside the D7-brane, contributes like a dissipationless system. The longitudinal conductivity involves only the first component. This is basically the same separation that was seen in the D4–D8 model (see (22.64), (22.65)).

This state of holographic matter exhibits a variety of other interesting phenomena as a function of the charge density, temperature, background magnetic field, and mass.

Consider first the state at $T = 0$, $d = 0$, $b = 0$ and $m = 0$. In this case the D7-brane embedding is actually $AdS_4 \times S^2 \times S^2$, so this situation is described by a conformal field theory. Note that in this case $\sigma_{xx} \neq 0$. At non-zero density the system becomes unstable to the formation of stripes. The instability is signaled by the existence of a quasi-normal mode (in the transverse gauge field sector) with positive imaginary part in a finite range of momenta [71]. At a high enough temperature or high enough magnetic field this instability disappears. It is convenient to parametrize the situation with $\hat{b} = b/r_T^2$ and $\hat{d} = d/r_T^2$. Then the instability towards the striped phase at zero magnetic field and $m = 0$ happens for $\hat{d} > 5.5$. This is demonstrated in Fig. 22.13a. Above the quantum critical point ($T = m = d = 0$) there is a region which resembles a Fermi-like liquid, and on both sides there is a striped phase. For non-zero $\hat{b}$ and $m = 0$ the instability sets in at some other value of $\hat{d}$, as shown in Fig. 22.13b [72]. As m increases the instability sets in at a lower temperature.

The system also has a zero sound mode. At non-zero temperature the quasi-normal mode with the smallest imaginary part at low momentum is a purely dis-

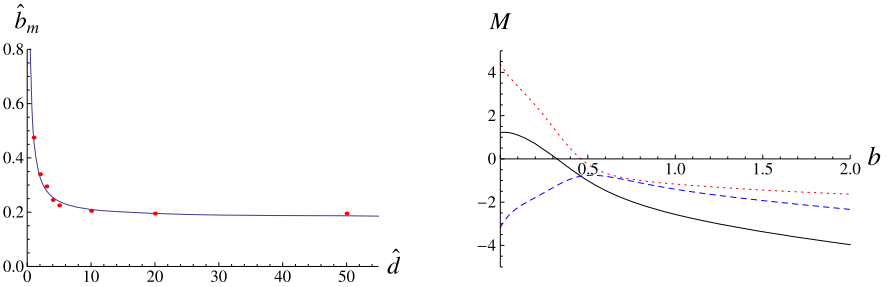

Fig. 22.14 (*Left*): The *line* in the $\hat{b}, \hat{d}$ plane for $m = 0$, separating the situation when the zero-sound is gapped (*above the line*) and the situation when it is gapless (*below the line*). (*Right*): The magnetization as a function of magnetic field (*solid line*) and the individual contributions from the DBI (*dashed line*) and the CS term (*pointed line*) for $m = 1$ $d = 1$ and $r_T = 0.1$

sipative hydrodynamical mode ($\omega(k = 0) = 0$). At some non-zero momentum it meets another purely dissipative mode (ω purely imaginary) and crosses from a hydrodynamical regime into a collisionless regime, where the resulting complex mode can be identified with the finite temperature zero-sound mode [71] (see also [73]). The zero sound mode becomes massive as the magnetic field crosses a critical value [72, 74] (Fig. 22.14a).

For $m \neq 0$ the system can have a non-zero transverse conductivity, even at zero magnetic field. This is due to having a non-trivial $c(r)$ for these embeddings. This is reminiscent of the anomalous Hall effect (AHE) that appears in ferromagnetic materials (for a review see [75]). Indeed for $m \neq 0$ the system is ferromagnetic (Fig. 22.14b) due to the second term in (22.82). Note that both the AHE and the ferromagnetic behavior, as well as the instability towards a striped phase, have a common origin in the Chern-Simon term $\int dr\, c(r) F \wedge F$ in the brane action.

Acknowledgements O.B. and G.L. would like to thank Matt Lippert and Niko Jokela, who were an integral part in all our work on the models reviewed in Sects. 22.3 and 22.4. O.B. also thanks the Aspen Center for Physics, where this work was completed, for its hospitality. J.E. would like to thank her collaborators Martin Ammon, Matthias Kaminski, Patrick Kerner, René Meyer, Jonathan Shock and Migael Strydom, involved in the joint work presented in Sect. 22.2. This work was supported in part by the Israel Science Foundation under grant No. 392/09, and in part by the US-Israel Binational Science Foundation under grant No. 2008-072.

References

1. V.P. Gusynin, V.A. Miransky, I.A. Shovkovy, Catalysis of dynamical flavor symmetry breaking by a magnetic field in $(2 + 1)$-dimensions. Phys. Rev. Lett. **73**, 3499–3502 (1994)
2. V.P. Gusynin, V.A. Miransky, I.A. Shovkovy, Dimensional reduction and dynamical chiral symmetry breaking by a magnetic field in $(3 + 1)$-dimensions. Phys. Lett. B **349**, 477–483 (1995)
3. V.A. Miransky, I.A. Shovkovy, Magnetic catalysis and anisotropic confinement in QCD. Phys. Rev. D **66**, 045006 (2002)

4. D.T. Son, M.A. Stephanov, Axial anomaly and magnetism of nuclear and quark matter. Phys. Rev. D **77**, 014021 (2008)
5. K. Fukushima, D.E. Kharzeev, H.J. Warringa, The chiral magnetic effect. Phys. Rev. D **78**, 074033 (2008)
6. M.N. Chernodub, Superconductivity of QCD vacuum in strong magnetic field. Phys. Rev. D **82**, 085011 (2010)
7. M.N. Chernodub, Spontaneous electromagnetic superconductivity of vacuum in strong magnetic field: evidence from the Nambu–Jona-Lasinio model. Phys. Rev. Lett. **106**, 142003 (2011)
8. D.C. Tsui, H.L. Stormer, A.C. Gossard, Two-dimensional magnetotransport in the extreme quantum limit. Phys. Rev. Lett. **48**, 1559–1562 (1982)
9. R.B. Laughlin, Anomalous quantum Hall effect—an incompressible quantum fluid with fractionally charged excitations. Phys. Rev. Lett. **50**, 1395–1398 (1983)
10. A. Karch, E. Katz, Adding flavor to AdS/CFT. J. High Energy Phys. **0206**, 043 (2002)
11. T. Sakai, S. Sugimoto, Low energy hadron physics in holographic QCD. Prog. Theor. Phys. **113**, 843–882 (2005)
12. S.-J. Rey, Talk given at Strings 2007 in Madrid, 2007
13. S.-J. Rey, String theory on thin semiconductors: holographic realization of Fermi points and surfaces. Prog. Theor. Phys. Suppl. **177**, 128–142 (2009)
14. J.L. Davis, P. Kraus, A. Shah, Gravity dual of a quantum Hall plateau transition. J. High Energy Phys. **0811**, 020 (2008)
15. O. Bergman, N. Jokela, G. Lifschytz, M. Lippert, Quantum Hall effect in a holographic model. J. High Energy Phys. **1010**, 063 (2010)
16. K. Jensen, A. Karch, D.T. Son, E.G. Thompson, Holographic Berezinskii-Kosterlitz-Thouless transitions. Phys. Rev. Lett. **105**, 041601 (2010)
17. N. Evans, A. Gebauer, K.-Y. Kim, M. Magou, Phase diagram of the D3/D5 system in a magnetic field and a BKT transition. Phys. Lett. B **698**, 91–95 (2011)
18. J.M. Maldacena, The large N limit of superconformal field theories and supergravity. Adv. Theor. Math. Phys. **2**, 231–252 (1998)
19. J. Erdmenger, N. Evans, I. Kirsch, E. Threlfall, Mesons in gauge/gravity duals—a review. Eur. Phys. J. A **35**, 81–133 (2008)
20. M. Kruczenski, D. Mateos, R.C. Myers, D.J. Winters, Meson spectroscopy in AdS/CFT with flavor. J. High Energy Phys. **0307**, 049 (2003)
21. J. Babington, J. Erdmenger, N.J. Evans, Z. Guralnik, I. Kirsch, Chiral symmetry breaking and pions in nonsupersymmetric gauge/gravity duals. Phys. Rev. D **69**, 066007 (2004)
22. V.G. Filev, C.V. Johnson, R.C. Rashkov, K.S. Viswanathan, Flavoured large N gauge theory in an external magnetic field. J. High Energy Phys. **0710**, 019 (2007)
23. J. Erdmenger, R. Meyer, J.P. Shock, AdS/CFT with flavour in electric and magnetic Kalb-Ramond fields. J. High Energy Phys. **0712**, 091 (2007)
24. V.G. Filev, R.C. Raskov, Magnetic catalysis of chiral symmetry breaking. A holographic prospective. Adv. High Energy Phys. **2010**, 473206 (2010)
25. V.G. Filev, D. Zoakos, Towards unquenched holographic magnetic catalysis. J. High Energy Phys. **1108**, 022 (2011)
26. J. Erdmenger, V.G. Filev, D. Zoakos, Magnetic catalysis with massive dynamical flavours (2011)
27. M. Ammon, V.G. Filev, J. Tarrio, D. Zoakos, D3/D7 quark-gluon plasma with magnetically induced anisotropy. J. High Energy Phys. **1209**, 039 (2012)
28. N. Evans, T. Kalaydzhyan, K.-y. Kim, I. Kirsch, Non-equilibrium physics at a holographic chiral phase transition. J. High Energy Phys. **1101**, 050 (2011)
29. N. Evans, A. Gebauer, K.-Y. Kim, M. Magou, Holographic description of the phase diagram of a chiral symmetry breaking gauge theory. J. High Energy Phys. **1003**, 132 (2010)
30. K. Jensen, A. Karch, E.G. Thompson, A holographic quantum critical point at finite magnetic field and finite density. J. High Energy Phys. **1005**, 015 (2010)

31. N. Evans, A. Gebauer, K.-Y. Kim, E, B, μ, T phase structure of the D3/D7 holographic dual. J. High Energy Phys. **1105**, 067 (2011)
32. M. Ammon, J. Erdmenger, M. Kaminski, P. Kerner, Superconductivity from gauge/gravity duality with flavor. Phys. Lett. B **680**, 516–520 (2009)
33. M. Ammon, J. Erdmenger, M. Kaminski, P. Kerner, Flavor superconductivity from gauge/gravity duality. J. High Energy Phys. **0910**, 067 (2009)
34. O. Aharony, K. Peeters, J. Sonnenschein, M. Zamaklar, Rho meson condensation at finite isospin chemical potential in a holographic model for QCD. J. High Energy Phys. **0802**, 071 (2008)
35. A. Rebhan, A. Schmitt, S.A. Stricker, Meson supercurrents and the Meissner effect in the Sakai-Sugimoto model. J. High Energy Phys. **0905**, 084 (2009)
36. J. Erdmenger, P. Kerner, M. Strydom, Holographic superconductors at finite isospin density or in an external magnetic field. PoS **FacesQCD**, 004 (2010)
37. M. Ammon, J. Erdmenger, P. Kerner, M. Strydom, Black hole instability induced by a magnetic field. Phys. Lett. B **706**, 94–99 (2011)
38. A. O'Bannon, Hall conductivity of flavor fields from AdS/CFT. Phys. Rev. D **76**, 086007 (2007)
39. Y.-Y. Bu, J. Erdmenger, J.P. Shock, M. Strydom, Magnetic field induced lattice ground states from holography. J. High Energy Phys. **1303**, 165 (2013)
40. V.V. Braguta, P.V. Buividovich, M.N. Chernodub, A.Yu. Kotov, M.I. Polikarpov, Electromagnetic superconductivity of vacuum induced by strong magnetic field: numerical evidence in lattice gauge theory. Phys. Lett. B **718**, 667–671 (2012)
41. J. Ambjorn, P. Olesen, Electroweak magnetism: theory and application. Int. J. Mod. Phys. A **5**, 4525–4558 (1990)
42. N. Callebaut, D. Dudal, H. Verschelde, Holographic study of rho meson mass in an external magnetic field: paving the road towards a magnetically induced superconducting QCD vacuum? PoS **FacesQCD**, 046 (2010)
43. N. Callebaut, D. Dudal, H. Verschelde, Holographic rho mesons in an external magnetic field. J. High Energy Phys. **1303**, 033 (2013)
44. E. Witten, Anti-de Sitter space, thermal phase transition, and confinement in gauge theories. Adv. Theor. Math. Phys. **2**, 505–532 (1998)
45. H. Hata, T. Sakai, S. Sugimoto, S. Yamato, Baryons from instantons in holographic QCD. Prog. Theor. Phys. **117**, 1157 (2007)
46. O. Aharony, J. Sonnenschein, S. Yankielowicz, A holographic model of deconfinement and chiral symmetry restoration. Ann. Phys. **322**, 1420–1443 (2007)
47. O. Bergman, G. Lifschytz, Holographic $U(1)_A$ and string creation. J. High Energy Phys. **0704**, 043 (2007)
48. O. Bergman, G. Lifschytz, M. Lippert, Holographic nuclear physics. J. High Energy Phys. **0711**, 056 (2007)
49. J.L. Davis, M. Gutperle, P. Kraus, I. Sachs, Stringy NJL and Gross-Neveu models at finite density and temperature. J. High Energy Phys. **0710**, 049 (2007)
50. M. Rozali, H.-H. Shieh, M. Van Raamsdonk, J. Wu, Cold nuclear matter in holographic QCD. J. High Energy Phys. **0801**, 053 (2008)
51. O. Bergman, G. Lifschytz, M. Lippert, Response of holographic QCD to electric and magnetic fields. J. High Energy Phys. **0805**, 007 (2008)
52. C.V. Johnson, A. Kundu, External fields and chiral symmetry breaking in the Sakai-Sugimoto model. J. High Energy Phys. **0812**, 053 (2008)
53. F. Preis, A. Rebhan, A. Schmitt, Inverse magnetic catalysis in dense holographic matter. J. High Energy Phys. **1103**, 033 (2011)
54. F. Preis, A. Rebhan, A. Schmitt, Holographic baryonic matter in a background magnetic field. J. Phys. G **39**, 054006 (2012)
55. C.V. Johnson, A. Kundu, Meson spectra and magnetic fields in the Sakai-Sugimoto model. J. High Energy Phys. **0907**, 103 (2009)

56. M.A. Metlitski, A.R. Zhitnitsky, Anomalous axion interactions and topological currents in dense matter. Phys. Rev. D **72**, 045011 (2005)
57. G.M. Newman, D.T. Son, Response of strongly-interacting matter to magnetic field: some exact results. Phys. Rev. D **73**, 045006 (2006)
58. C. Hoyos, T. Nishioka, A. O'Bannon, A chiral magnetic effect from AdS/CFT with flavor. J. High Energy Phys. **1110**, 084 (2011)
59. O. Bergman, G. Lifschytz, M. Lippert, Magnetic properties of dense holographic QCD. Phys. Rev. D **79**, 105024 (2009)
60. A. Rebhan, A. Schmitt, S.A. Stricker, Anomalies and the chiral magnetic effect in the Sakai-Sugimoto model. J. High Energy Phys. **1001**, 026 (2010)
61. A. Rebhan, A. Schmitt, S. Stricker, Holographic chiral currents in a magnetic field. Prog. Theor. Phys. Suppl. **186**, 463–470 (2010)
62. E.G. Thompson, D.T. Son, Magnetized baryonic matter in holographic QCD. Phys. Rev. D **78**, 066007 (2008)
63. G. Lifschytz, M. Lippert, Holographic magnetic phase transition. Phys. Rev. D **80**, 066007 (2009)
64. G. Lifschytz, M. Lippert, Anomalous conductivity in holographic QCD. Phys. Rev. D **80**, 066005 (2009)
65. N. Jokela, M. Jarvinen, M. Lippert, A holographic quantum Hall model at integer filling. J. High Energy Phys. **1105**, 101 (2011)
66. R.C. Myers, M.C. Wapler, Transport properties of holographic defects. J. High Energy Phys. **0812**, 115 (2008)
67. N. Jokela, G. Lifschytz, M. Lippert, Magneto-roton excitation in a holographic quantum Hall fluid. J. High Energy Phys. **1102**, 104 (2011)
68. N. Jokela, M. Jarvinen, M. Lippert, Fluctuations of a holographic quantum Hall fluid. J. High Energy Phys. **1201**, 072 (2012)
69. S.M. Girvin, A.H. MacDonald, P.M. Platzman, Magneto-roton theory of collective excitations in the fractional quantum Hall effect. Phys. Rev. B **33**, 2481–2494 (1986)
70. A. Karch, A. O'Bannon, Metallic AdS/CFT. J. High Energy Phys. **0709**, 024 (2007)
71. O. Bergman, N. Jokela, G. Lifschytz, M. Lippert, Striped instability of a holographic Fermi-like liquid. J. High Energy Phys. **1110**, 034 (2011)
72. N. Jokela, G. Lifschytz, M. Lippert, Magnetic effects in a holographic Fermi-like liquid. J. High Energy Phys. **1205**, 105 (2012)
73. R.A. Davison, A.O. Starinets, Holographic zero sound at finite temperature. Phys. Rev. D **85**, 026004 (2012)
74. M. Goykhman, A. Parnachev, J. Zaanen, Fluctuations in finite density holographic quantum liquids. J. High Energy Phys. **1210**, 045 (2012)
75. N. Nagaosa, J. Sinova, S. Onoda, A.H. MacDonald, N.P. Ong, Anomalous Hall effect. Rev. Mod. Phys. **82**, 1539–1592 (2010)